Available online at www.sciencedirect.com

SciVerse ScienceDirect

Geochimica et Cosmochimica Acta 108 (2013) 45–62

Geochimica et Cosmochimica Acta

www.elsevier.com/locate/gca

Compositional and petrographic similarities of CV and CK chondrites: A single group with variations in textures and volatile concentrations attributable to impact heating, crushing and oxidation

John T. Wasson *, Junko Isa, Alan E. Rubin

Institute of Geophysics and Planetary Physics, Department of Earth and Space Sciences and Department of Chemistry and Biochemistry, University of California, Los Angeles, CA 90095-1567, USA

Received 14 July 2012; accepted in revised form 11 January 2013; available online 25 January 2013

Abstract

Greenwood et al. (2010) gathered data on O-isotopic and elemental compositions and reevaluated literature data for CV and CK chondrites. They concluded that these two chondrite groups originated on the same parent asteroid, with CK chondrites being metamorphosed CV chondrites (which are otherwise missing types 4 through 6). To test this interpretation we have gathered new instrumental neutron-activation-analysis (INAA) data for CV and CK chondrites and reexamined their petrographic features. The new INAA data like the older data show scatter attributable to weathering effects, but we conclude that the refractory lithophile abundances are the same in CV and CK, in agreement with the Greenwood et al. interpretation. Several volatile elements are significantly lower in CK than in CV chondrites. Among the elements we determine, the greatest difference between CV and CK is found for Br, for which the CV/CK ratio is ~4; As and Sb are about 20% lower in CK than CV and smaller differences are observed for Zn, Ga and Se. It seems likely that volatiles were lost during impact-heating events that also provided the heat responsible for metamorphic recrystallization. Within statistical uncertainty, chondrules in CV and CK chondrites are the same size and have similar textural distributions. A significant petrographic difference between CK and CV chondrites cited by Kallemeyn et al. (1991) was the much higher percentage of igneous rims around CV chondrules. However, we now recognize that many chondrules in CK3.8 NWA 1559 have igneous rims and in CK4 chondrites, igneous rims are recognizable by their associated sulfide-rich rings; there are no quantifiable CV–CK differences in igneous-rim abundances. We used Ca and Al maps to show that CK chondrites have CAI abundances similar to those of CV chondrites. It thus appears that there are no resolvable pre-metamorphic petrographic differences between CV and CK chondrites. We recommend that the "CK" designation be abandoned and that the CV group be acknowledged as spanning the range of petrologic types 3–6. We suggest that CK3 chondrites be designated $CV3_{OxK}$. Most CK4 chondrites are highly fragmental; collisional crushing appears to be much more common than in CV chondrites. It seems likely that CK chondrites formed from reduced CV3 materials after the latter was impacted, buried, aqueously altered and annealed.

1. INTRODUCTION

The CK group was first defined by Kallemeyn et al. (1991) based on INAA (instrumental-neutron-activation-analysis) data and petrographic observations; they noted its close compositional and textural relationship to CV chondrites, but concluded that the two sets form distinguishable groups on the basis of differing refractory lithophile abundances and textural features (specifically, higher CV abundances of refractory inclusions and coarse-grained igneous rims around chondrules).

* Corresponding author.
E-mail address: jtwasson@ucla.edu (J.T. Wasson).

0016-7037/$ - see front matter © 2013 Elsevier Ltd. All rights reserved.
http://dx.doi.org/10.1016/j.gca.2013.01.011

Huber et al. (2006) took advantage of the increase in the availability of CK samples resulting from recoveries from hot and cold deserts and analyzed a set of samples by INAA and petrographic techniques. However, even though they chose relatively unweathered meteorites, they found that many CK chondrites had experienced strong weathering effects; especially affected are the siderophiles and chalcophiles Ni, Co, Se and Zn in CK chondrites from hot deserts.

Greenwood et al. (2010) measured precise O-isotopic compositions in sets of CV and CK chondrites and gathered compositional data for 16 elements using ICP-MS (inductively-coupled-plasma mass spectrometry); they noted that the isotopic, elemental and petrographic properties of CV and CK chondrites are so closely similar that it is best to conclude that they are members of a single chondrite group differing only in their degree of thermal metamorphism. They noted that apparent differences in CAI abundances, chondrule sizes and the presence/absence of coarse igneous rims around chondrules (Fig. 1a–c) could reflect metamorphic effects, with rims and CAIs tending to be texturally unresolvable from matrix after moderate metamorphism. This view also offered a satisfying explanation for the absence of higher (4 through 6) petrographic types among CV chondrites. (Such types are, of course, present in ordinary, enstatite and R chondrites.)

There is no doubt that CK and CV chondrites are closely related and that there are no documented examples of CV chondrites of petrographic type $\geqslant 4$. It therefore seemed important that we analyze additional CV and CK samples using INAA and petrography to test the Greenwood et al. (2010) interpretation. The abstract by Isa et al. (2011) indicates that these workers are pursuing a similar theme; they noted that concentrations of Tl and Bi are much higher in CV than in CK chondrites, a fact that they interpreted as indicating that the groups had different nebular origins.

2. EXPERIMENTAL TECHNIQUES AND SAMPLES

2.1. Neutron activation techniques

Our INAA techniques are closely similar to those of Choe et al. (2010). Samples with masses in the range of 250–320 mg were analyzed as a few chips or (preferably) as blocks ~3 mm thick. Nuclides with half-lives ranging from hours to years were analyzed in four successive counting periods. With few exceptions, the meteorites were analyzed in duplicate in separate irradiations. By analyzing duplicate samples we obtain information about both analytical and sampling errors, and occasionally catch more egregious problems such as mislabeling of samples.

Samples were irradiated for 3 h in the lazy susan of the Triga Mark I reactor at the University of California, Irvine; the neutron flux was about 0.8×10^{12} neutrons cm^{-2} s^{-1}. Standards were meteorites and USGS rock powders (this contrasts with the earlier studies by Kallemeyn and coworkers in which the standards were evaporated aliquots of calibrated aqueous solutions). All irradiations included a

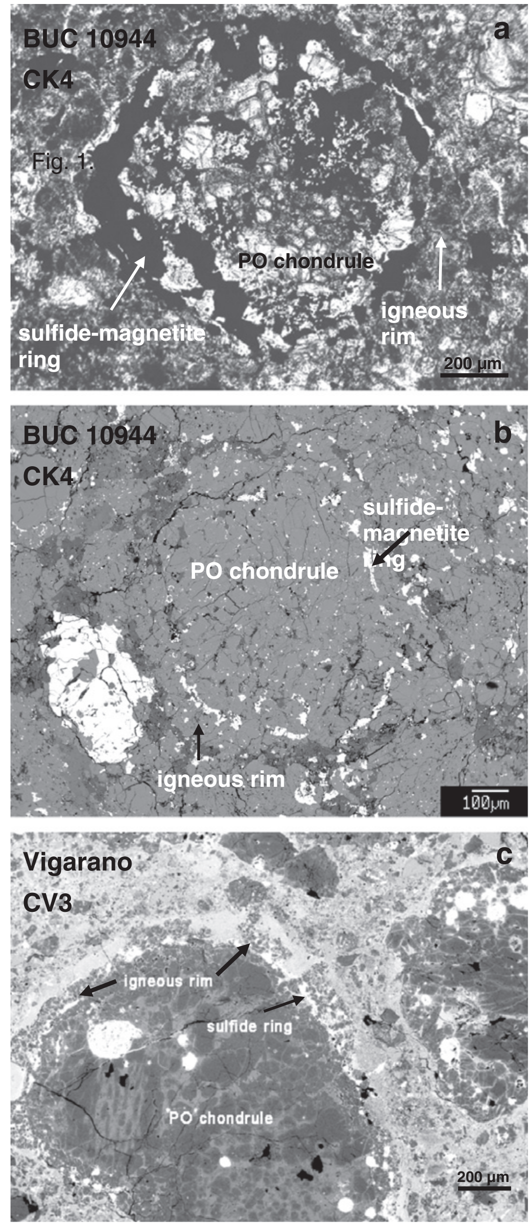

Fig. 1. (a) Porphyritic olivine–pyroxene (POP) chondrule in CK4 BUC 10944 showing a broad, uneven sulfide–magnetite ring (black) surrounded by a coarse-grained, recrystallized igneous rim. The igneous rim is difficult to distinguish from the surrounding meteorite matrix but appears a little darker. Transmitted light. (b) Porphyritic olivine (PO) chondrule in BUC 10944 with a thin, discontinuous sulfide–magnetite ring (white to light gray). The surrounding coarse-grained, recrystallized igneous rim is separated from the matrix by plagioclase grains (dark gray) in the matrix in the chondrule vicinity. A large silicate-bearing sulfide grain, unassociated with the chondrule, occurs at lower left. Backscattered electron (BSE) image. (c) Enveloping compound chondrule in $CV3_R$ Vigarano containing a large PO primary and an enclosed barred olivine (BO) secondary (lower left). The primary chondrule is surrounded by a thin sulfide ring (white), beyond which lies a discontinuous igneous rim (medium gray). Fine-grained FeO-rich matrix (smooth light-gray region) partly surrounds the igneous rim. The sulfide ring is similar to that around the PO chondrule in CK4 BUC 10944 in Fig. 1b. BSE image.

portion of the UCLA CV3 Allende standard powder, a small (ca. 90 mg) piece of the Filomena IIAB iron meteorite, and portions of the USGS SCo-1 and BHVO-1 powders. In one run we included NBS iron 809b as an Sb standard; samples of the Smithsonian Institution Allende standard powders s3 p4 and s3 p18 were each included in one irradiation.

2.2. Choice of samples; weathering effects in CK chondrites

Table 1 provides information about the samples analyzed in the present study. There are only two CK chondrite falls, one of which (Kobe) is not available in sufficient quantities for us to analyze. Among the seven observed-fall CV chondrites, Kallemeyn and Wasson (1981) analyzed four (Allende, Bali, Mokoia and Vigarano). Kallemeyn and Wasson (1982) later analyzed the Grosnaja fall but obtained discrepant data and designated it an anomalous CV.

Because weathering effects have seriously degraded all CK finds and some CV finds from hot deserts, we have limited our new CK and CV sample sets to relatively unweathered recoveries from Antarctica. As shown in Table 1 three CV and three CK samples are weathering grade B with the remainder listed as A or A/B. Nonetheless, we will show that some CK finds from Antarctica also show serious elemental fractionations that we attribute to terrestrial weathering.

The CV chondrites fall into three subgroups varying in their degree of oxidation: the reduced ($CV3_R$) subgroup that includes Vigarano, Leoville, Efremovka and Arch, the oxidized Allende-like ($CV3_{OxA}$) subgroup, and the oxidized Bali-like ($CV3_{OxB}$) subgroup (Weisberg et al., 1997; Krot et al., 2005). Nevertheless, individual CV chondrites contain millimeter-to-centimeter-size regions that differ in subtype from the main lithology: e.g., $CV3_{OxB}$ material occurs in $CV3_R$ Vigarano (Krot et al., 2000), incompletely characterized $CV3_{Ox}$ oxidized material occurs in $CV3_R$ Leoville (McSween, 1977a) and both $CV3_{OxA}$ and $CV3_{OxB}$ material occur in Mokoia (Krot et al., 1998b).

Our new CV samples represent all three subgroups (as determined by their relative abundances of magnetite, Ni-bearing sulfide and metallic Fe–Ni): GRA 06101 ($CV3_{OxA}$), LAP 02206 ($CV3_{OxA}$), MIL 07002 ($CV3_{OxA}$), MCY 05219 ($CV3_{OxB}$), RBT 04143 ($CV3_{OxA}$), and Y 981208 ($CV3_R$).

We also analyzed MIL 090001 based on a report that it was a CV2 (Keller et al., 2011). However, our analysis showed it not to be a CV but to have a CR-like composition, consistent with subsequent petrographic observations (Keller et al., 2012). We include data for MIL 090001 and a brief discussion of its reclassification as CR2. We also reanalyzed the ungrouped C3 chondrite Ningqiang that earlier papers had designated CV-an (Rubin et al., 1988), CK-an (Kallemeyn et al., 1991), an ungrouped carbonaceous chondrite (Kallemeyn, 1996), or a meteorite “closely related to oxidized CV3 chondrites” (Weisberg et al., 1996).

Table 1
Sources of whole-rock samples and thin sections.

Group, type	Wth*	Meteorite	Abbrev.	Source	Thin sect.	Notes
CV3	Fall	Allende SI s3		SI powders	- -	s3 p4 and s3 p18
CV3	Fall	Allende UCLA		UCLA powder	- -	
CV3	B	GRA 06101,36		MWG, JSC	,41	
CV3	B	LAP 02206,31	LAP02	MWG, JSC	,35	
CV3	A/Be	MIL 07002,12		MWG, JSC	,15	
CV3	B	MCY 05219,8		MWG, JSC	,11	
CV3	A/B	RBT 04143,8	RBT04	MWG, JSC	,10	
CV3	A	Y 981208		NIPR	,51-2	
CK4	Ae	ALH 84038		MWG, JSC	,4	
CK4	A/B	BUC 10944,5	BUC	MWG, JSC	,8	
CK5	A/Be	EET 92002	EET	MWG, JSC		and EET87526,9
CK4	Fall	Karoonda	Kar	AMNH	USNM 904-2	
CK5	B	LAP 03784	LAP03	MWG, JSC	,12	
CK5	A/B	LAP 10030,6	LAP10	MWG, JSC	,9	
CK4	A/B	LAR 04318	LAR	MWG, JSC	,11	
CK4	W3	Lucerne Valley 101		UCLA	1959	
CK6	B	MIL 090103,7	MIL09	MWG, JSC	,9 and,6	
CK5	wi2	NWA 060		UCLA	851	
CK4	W1	NWA 521		UCLA	1071	
CK3.8	wi3	NWA 1559		NHMV	LMT 34	
CK4	wi2	NWA 5025		UCLA	1935	
CK5	B	RBT 03522	RBT03	MWG, JSC	,10	
Cungr3	Fall	Ningqiang	NQ	UCLA	420–422	
CR2	B	MIL 090001		MWG, JSC	,12	

* *Abbreviations:* abbrev., abbreviations used on figures; wth, weathering class as reported in the Meteoritical Bulletin except for NWA 060, 1559 and 5025, this study; MWG, JSC, Meteorite Working Group, Johnson Spacecraft Center; NIPR, National Institute of Polar Research, Tokyo; AMNH, American Museum of Natural History, New York; USNM, U.S. National Museum of the Smithsonian Institution; NHMV, Naturhistorisches Museum, Vienna; USNM, US National Museum, Smithsonian Institution.

Table 2
Means and standard deviations for analyses of the UCLA Allende standard powder for the period August 2009 through February 2012.

Element	Na (mg/g)	K (μg/g)	Ca (mg/g)	Sc (μg/g)	Cr (mg/g)	Mn (mg/g)	Fe (mg/g)	Co (μg/g)	Ni (mg/g)	Zn (μg/g)	Ga (μg/g)	As (μg/g)
Mean	3.36	286	17.8	10.9	3.65	1.46	237	666	13.6	117.4	6.09	1.59
Stan dev	0.14	15	1.0	0.15	0.05	0.02	6.6	18	0.6	4.9	0.50	0.09
Rel stan dev (%)	4.2	5.4	5.6	1.4	1.2	1.4	2.8	2.8	4.2	4.2	8.1	5.8
Element	Se (μg/g)	Br (μg/g)	Ru (μg/g)	Sb (ng/g)	La (ng/g)	Sm (ng/g)	Eu (ng/g)	Yb (ng/g)	Lu (ng/g)	Os (ng/g)	Ir (ng/g)	Au (ng/g)
Mean	8.27	1.62	1.10	85	499	308	115	320	45	812	757	146
Stan dev	0.11	0.01	0.03	5	28	15	12	15	3	35	27	6
Rel stan dev (%)	1.3	0.8	3.0	6.4	5.6	4.8	11	4.8	6.9	4.4	3.6	4.4

2.3. Petrographic techniques

In Table 1 we list the thin sections that we studied. Thin sections were examined in transmitted and reflected light with an Olympus BX60 petrographic microscope. Sizes were measured microscopically with a calibrated reticle. Backscattered-electron (BSE) images were made with the JEOL electron microprobe at UCLA. Grain sizes based on these BSE images typically include measurements of ∼20 grains normalized to the scale bar generated by the image software. Average grain sizes have an approximate uncertainty of ±4 μm. An RGB map (Mg–Ca–Al) was made of a 9-mm^2 area of a thin section of CK4 Karoonda using the JEOL probe (available in an Electronic annex to this article). Abundances of Ca- and Al-rich areas in this map were determined using Adobe Photoshop software.

3. RESULTS

3.1. Precision of INAA

As a measure of the precision of our results we list in Table 2 mean compositions and standard deviations measured in our UCLA Allende standard powder. Because this is a relatively uniform powder and because it is one of the standards, these standard deviations offer lower limits for the variance of our samples. Our relative standard deviations for the UCLA Allende powder are <3% for Sc, Cr, Mn, Fe, Co, Se and Br, 6–11% for Ga, Sb, Eu, Yb, Lu and Os, and 3–6% for the remaining elements.

3.2. New INAA results

Our chondrite data are listed in Table 3. We determined 24 elements in sets of seven CK and seven CV chondrites. All data are means of two or more analyses of 300-mg samples; individual analyses are available in the Electronic annex. All chondrites are finds from Antarctica except for the falls CK4 Karoonda and CV3 Allende. We also included a sample of the CK3-an Ningqiang fall and CR2 MIL 090001. We do not have data for Al and Mg in the samples.

3.3. Petrography

3.3.1. CK whole-rock crushing

Back-scattered electron images of typical matrix-rich regions of a suite of CK chondrites (petrologic types 3.8 to 5) show that these rocks consist mainly of small angular silicate grains (Fig. 2a–f) that appear to have been derived from crushed chondrules. Some coarser chondrule fragments are also present. The angular silicate grains are separated by irregular pore spaces. Many of the silicate grains contain internal fractures (e.g., Fig. 2d–f), readily visible in the images at high magnification. The finest-grained sample is CK3.8 NWA 1559 (Fig. 2a), the least-recrystallized member of the suite; silicate grain sizes in this rock range from ∼6 to 75 μm and average ∼11 μm. The Karoonda CK4 fall is highly fragmental with an average grain size of ∼20 μm (Fig. 2b). CK4 NWA 5025 is somewhat coarser, with an average grain size of ∼35 μm (Fig. 2c). The coarsest-grained sample among these six is CK5 LAP 10030 (Fig. 2f), the most extensively recrystallized member of the set. Its silicate grains have a roughly bimodal size distribution: there are many small grains ranging from 6 to 16 μm; larger grains typically range from ∼75 to 150 μm. The average grain size of LAP 10030 is on the order of 50–60 μm.

Not all CK chondrites appear to have been crushed to the same extent: we found that CK4 BUC 10944 (Fig. 3a), CK4-an Tanezrouft 057, CK4 NWA 521 (Fig. 3b), CK5 NWA 060 (Fig. 3c) and CK6 MIL 090103 (Fig. 3d) have silicate grains that are rounder and more equant than those in the majority of CK4 chondrites. The silicate grains appear to be coarser in these samples (even in CK4 BUC 10944, Tanezrouft 057 and NWA 521) than in the majority of CK4 chondrites (Fig. 2). Nevertheless, there is evidence that these rocks also suffered shock damage: there are numerous fractures, large and small, in the silicate grains in NWA 060 (Fig. 3c) and MIL 090103 (Fig. 3d).

In summary, the majority of CK3.8 and CK4 samples have been crushed (Fig. 2) and thus differ dramatically in structure from CV3 chondrites. For example, thin sections of CV3$_{OxA}$ Allende (e.g., Fig. 7.9 of Norton, 2002; p. 177 of Lauretta and Killgore, 2005) and CV3$_{OxA}$ Axtell (Fig. 7.16

Table 3
Concentrations of 24 elements in CK and CV chondrites determined by INAA. Also listed are data for Cungr3 Ningqiang and for CV2 MIL 09001.

	Na (mg/g)	K (μg/g)	Ca (mg/g)	Sc (μg/g)	Cr (mg/g)	Mn (mg/g)	Fe (mg/g)	Co (μg/g)	Ni (mg/g)	Zn (μg/g)	Ga (μg/g)	As (μg/g)
CV chondrites												
LAP 02206,31	3.26	238	16.3	9.85	3.69	1.47	232	654	13.7	106	6.5	1.47
MCY 05219,8	3.40	328	18.7	9.99	3.44	1.44	220	611	12.5	110	6.2	1.29
RBT 04143,8	3.28	256	17.5	10.53	3.59	1.39	219	610	12.5	103	5.2	1.43
GRA 06101,36	2.45	238	15.4	9.27	3.34	1.39	224	639	13.4	94	5.5	1.54
MIL 07002,12	2.37	215	16.2	8.57	3.20	1.34	206	705	13.2	82	5.0	1.50
Allende UCLA	3.38	279	17.7	10.89	3.61	1.46	234	660	13.1	119	6.4	1.60
Allende SI s3	3.12	292	17.8	10.90	3.46	1.38	226	647	12.3	120	5.9	1.59
CK chondrites												
LAR 04318	3.14	303	13.6	8.89	3.10	1.35	207	837	19.5	77	6.10	1.37
EET92002	2.87	242	13.8	9.94	3.68	1.45	235	607	11.9	101	5.96	1.56
MIL 090103,7	3.33	256	18.0	12.00	3.74	1.50	237	614	9.9	101	5.50	1.33
RBT 03522	3.06	309	14.6	9.88	3.40	1.50	221	443	8.1	101	4.73	1.19
BUC 10944,5	3.08	263	16.2	10.50	3.60	1.48	238	630	12.0	86	5.48	1.40
LAP 10030,6	3.07	299	12.7	10.10	3.34	1.56	228	664	13.6	102	6.62	1.57
Karoonda.	2.99	191	17.4	11.60	3.74	1.40	242	720	15.0	98	6.02	0.94
Other chondrites												
Ningqiang	3.53	337	14.0	9.36	3.48	1.48	235	662	13.0	124	7.1	1.78
MIL 090001,14	0.97	200	13.5	7.54	3.33	1.82	214	682	12.0	62	4.8	1.50

	Se (μg/g)	Br (μg/g)	Ru (μg/g)	Sb (ng/g)	La (ng/g)	Sm (ng/g)	Eu (ng/g)	Yb (ng/g)	Lu (ng/g)	Os (ng/g)	Ir (ng/g)	Au (ng/g)
CV chondrites												
LAP 02206,31	7.8	1.2	1.16	76	467	290	110	300	44	720	680	143
MCY 05219,8	8.1	1.5	0.95	76	367	256	106	329	38	737	640	147
RBT 04143,8	7.2	1.3	1.11	71	520	301	119	284	41	667	640	140
GRA 06101,36	7.3	0.9	1.01	69	375	236	101	263	45	589	627	119
MIL 07002,12	7.5	1.1	1.02	74	410	234	94	321	43	642	583	143
Allende UCLA	8.3	1.6	1.12	83	474	305	111	321	43	819	740	141
Allende SI s3	8.0	1.9	0.98	87	481	295	120	335	50	831	769	144
CK chondrites												
LAR 04318	6.9	0.40	0.96	95	390	235	100	222	38	698	630	95
EET92002	7.5	0.41	1.21	72	438	267	95	286	40	950	725	141
MIL 090103,7	7.6	0.30	1.25	69	438	278	123	317	33	739	731	77
RBT 03522	5.3	0.20	1.27	64	388	261	112	277	41	759	704	141
BUC 10944,5	5.4	0.28	1.05	80	421	293	112	298	44	808	690	113
LAP 10030,6	5.7	0.54	0.96	65	393	237	92	318	46	704	652	74
Karoonda.	7.3	0.56	1.02	50	444	312	136	364	50	1003	832	158
Other chondrites												
Ningqiang	9.1	1.78	0.97	63	355	218	98	262	44	782	694	140
MIL 090001,14+	6.6	0.81	0.92	47	291	187	84	231	35	582	539	162

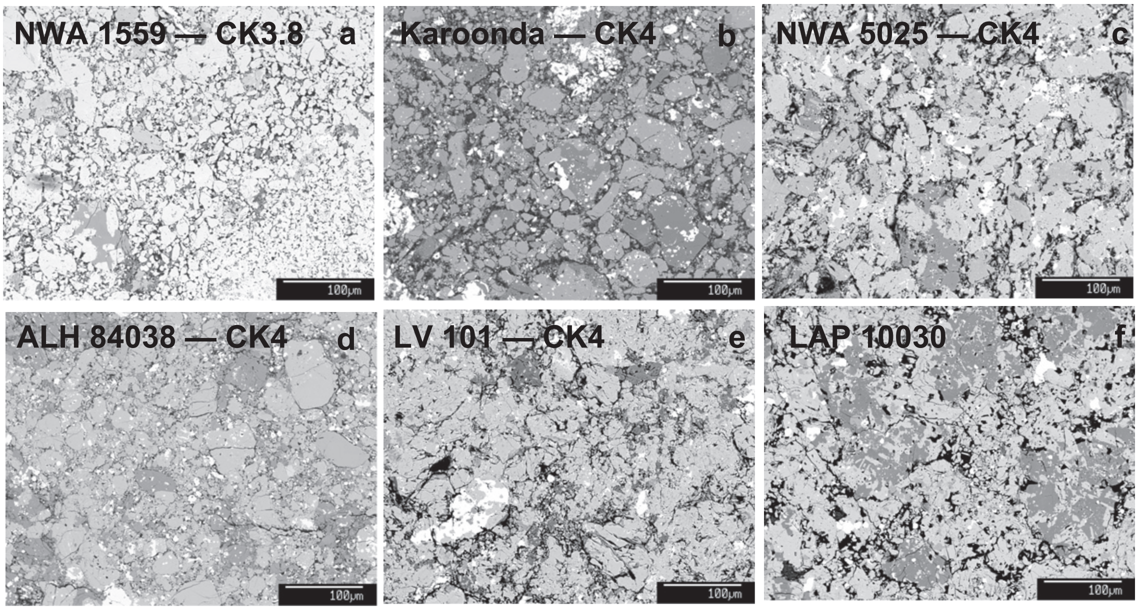

Fig. 2. A suite of CK chondrites ranging in petrologic type from 3.8 to 5 showing that the rocks consist mainly of angular silicate fragments. It is clear that the meteorites have experienced significant crushing, presumably due to impact processes. Many silicate grains are fractured in ALH 84038, LV 101 and LAP 10030. (a) NWA 1559, CK3.8. This sample appears finer-grained than the others, perhaps due to a lower degree of metamorphic recrystallization. (b) Karoonda, CK4. (c) NWA 5025, CK4. (d) ALH 84038, CK4. (e) Lucerne Valley 101, CK4. (f) LAP 10030, CK5. LAP 10030 is the coarsest grained of these samples, presumably due to more-extensive recrystallization. Olivine – light gray; orthopyroxene – medium gray; plagioclase – dark gray; sulfide and magnetite – white; fractures and pores – black. All of the images are at the same scale. BSE images.

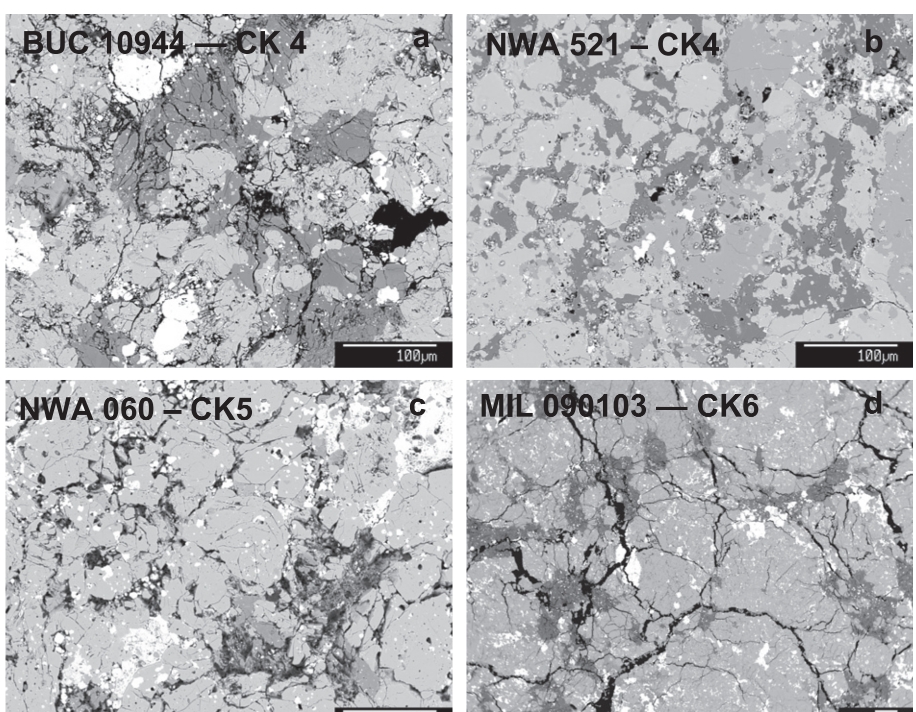

Fig. 3. Three CK chondrites that do not exhibit highly fragmental structures. (a) BUC 10944, CK4. Although there are small fragmental regions, the majority of silicate grains appear recrystallized. (b) NWA 521, CK4. Grains are coarser than in most CK4 chondrites; pore space seems limited. (c) NWA 060, CK5. There are coarse olivine grains in this meteorite that contain numerous fractures. (d) MIL 090103 CK6. This rock is significantly fractured; in addition to the large fractures separating grains, there are numerous small fractures inside the silicate grains. Olivine – light gray; orthopyroxene – medium gray; plagioclase – dark gray; sulfide and magnetite – white; fractures and pores – black. Note that MIL 090103 (Fig. 3d) is at a lower magnification than that of the other images. BSE images.

of Norton, 2002) show little evidence of crushing. Although many reduced CV3 chondrites have impact-induced foliations (e.g., Martin et al., 1975; Müller and Wlotzka, 1982; Kracher et al., 1985; Cain et al., 1986; Scott et al., 1992), they generally do not appear to have been extensively crushed (e.g., Leoville – Fig. 1 of Kracher et al., 1985; NWA 7107 – Fig. 4 of Rubin, 2012). There are too few observations to generalize about $CV3_{OxA}$ chondrites.

The CK5 chondrites, LAP 10030 (Fig. 2f) and NWA 060 (Fig. 3c), have crushed patches located between coarse silicate grains and assemblages. Although heavily fractured, CK6 MIL 090103 (Fig. 3d) contains few crushed regions.

3.3.2. Chondrules, igneous rims, CAIs and AOIs

CV3 and CK3 chondrites have indistinguishable mean chondrule apparent diameters (910 and 870 μm, respectively) (Rubin, 2010). Oxidized CV chondrites and CK chondrites have similar modal abundances of chondrules (McSween, 1977a; Rubin, 2010). Despite such petrologic similarities (which were known in broad outline in 1991), Kallemeyn et al. (1991) rejected the idea that CK chondrites are simply metamorphosed CV chondrites in part because of what these workers judged to be innate petrographic differences between the groups. Rubin (1984) had reported that ~50% of CV chondrules are surrounded by igneous rims, but Kallemeyn et al. (1991) found none around CK4 chondrules. Although McSween (1977a) had reported an average of ~5 vol.% CAIs in CV chondrites (later amended to 3.0 vol.% by Hezel et al., 2008), Kallemeyn et al. found CAIs to be very rare in CK chondrites (<1 vol.%), consistent with observations of Karoonda by McSween (1977b).

The question arises as to how to recognize igneous rims and CAIs in (metamorphosed) CK4 chondrites. Rubin (1984) reported that rings of sulfide commonly line the inner and outer boundaries of igneous rims around CV3 chondrules (e.g., Fig. 1c); i.e., they occur at the chondrule/rim and rim/matrix interfaces. Our new observations indicate that few, if any, CV3 chondrules lacking igneous rims are surrounded by sulfide rings. Thus, the presence of a sulfide-rich ring around a CK4 chondrule appears to be an indicator of the presence of an igneous rim. Because sulfide is generally associated with magnetite in CK chondrites (Rubin, 1993; Geiger and Bischoff, 1995), sulfide-rich rings around CK4 chondrules would be expected to contain magnetite. Fig. 1a, b show two porphyritic chondrules in CK4 BUC 10944, each of which is surrounded by a sulfide-magnetite ring. The surrounding olivine-rich igneous rim in each case is difficult to distinguish from the adjacent coarse olivine grains in the recrystallized matrix. [This observation is consistent with the coarseness of the olivine grains in the rim around an amoeboid olivine inclusion in CK3.8 NWA 1559 (a rock that is less metamorphosed than BUC 10944) (Fig. 4; Rubin, 2013).] About 40% of the chondrules in CK4 chondrites (18/46) are surrounded by sulfide-rich rings; we infer that the majority of these are surrounded by difficult-to-discern mafic-silicate-rich igneous rims. Kallemeyn et al. (1991) failed to recognize igneous rims around CK4 chondrules primarily because they had not realized that sulfide-rich rings are a marker for igneous rims.

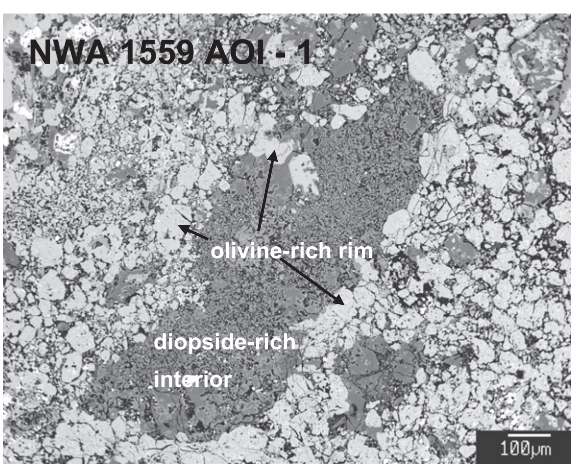

Fig. 4. An amoeboid olivine inclusion from CK3 NWA 1559 that has a coarse ferroan olivine rim enclosing a fine-grained diopside-rich porous interior. The rim is recrystallized and difficult to distinguish from coarse olivine grains in the meteorite matrix even though the whole rock (estimated to be petrologic type 3.8) is less metamorphosed than CK4 chondrites. BSE image.

At the time Kallemeyn et al. (1991) published their paper, only a single CAI in a CK4 had been described: a 1.6 × 2.2-mm-size fassaite-olivine-pleonaste-bearing inclusion in Karoonda (MacPherson and Delaney, 1985). Additional CAIs were subsequently reported in CK3 (e.g., Geiger et al., 1993; Ivanova et al., 2000; Zipfel et al., 2000; Brandstätter et al., 2003; Smith and Russell, 2003; Chaumard et al., 2009), CK4 (Keller, 1992; Keller et al., 1992; Noguchi, 1993; Greenwood et al., 2000a,b; Kurat et al., 2002; Neff and Righter, 2006; Chaumard et al., 2009, 2011), CK4/5 (Bukovanská et al., 2003), CK5 (Noguchi, 1993; Neff and Righter, 2006) and CK5/6 chondrites (Neff and Righter, 2006).

Identification and characterization of CK3 chondrites after the Kallemeyn et al. (1991) study showed that the less-metamorphosed CK samples have close petrographic ties to CV3 chondrites: Rubin (2010) found that 32 ± 6% of chondrules in CK3.8 NWA 1559 are surrounded by igneous rims; this is only marginally lower than the percentages in both CV3 Kaba and CV3 Vigarano (42 ± 6%; Rubin, 1984). Rubin (2011) estimated that CK3 chondrites contain ~4 vol.% CAIs, similar to the CV3 mean of 3 vol.% (Hezel et al., 2008).

We made a 9-mm^2 RGB (Mg–Ca–Al) map of a typical region of Karoonda (available in an Electronic annex to this article) and found that areas enriched in both Ca and Al (an upper limit on the approximate modal abundance of CAIs) constitute about 5–6 vol.% of this area of the thin section. However, the Ca- and Al-rich patches in Karoonda tend to be rather small (~40–70 μm), indicating that the CAIs have been crushed. Because the sizes were so small we did not obtain elemental data for these grains. These data imply that the apparent dearth of CAIs and of igneous rims around chondrules in the CK4 chondrites studied by

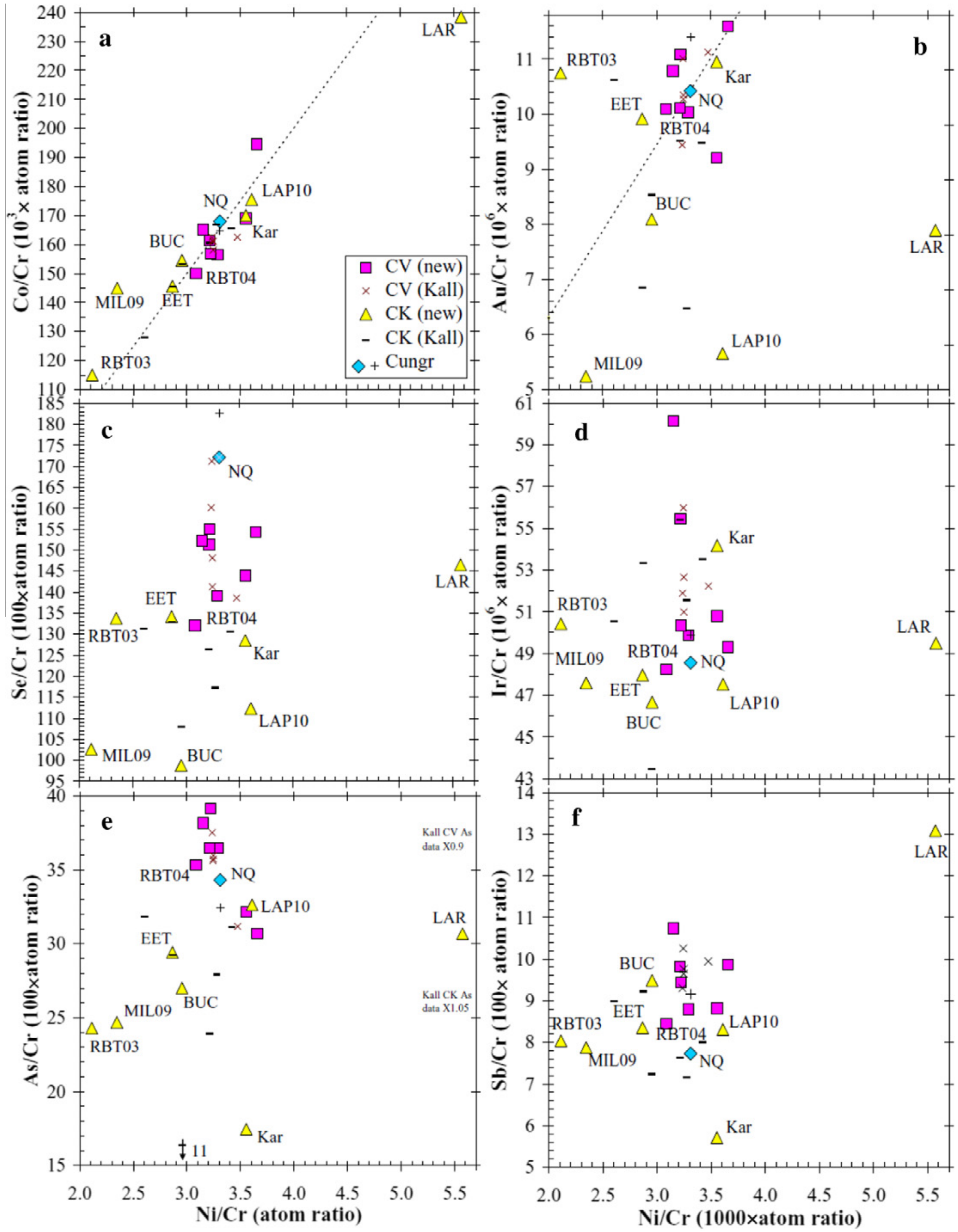

Fig. 5. Plots of the Cr-normalized abundances of the siderophiles Co, Au, Se, Ir, As and Sb against Ni. Scales are linear. With the exception of some outliers that appear to have experienced weathering or impact alteration, total ranges are relatively small; maximum/minimum ratios are about 1.3. The outliers are mainly CK chondrites; five of the CKs show severe fractionations among Co, Se and Au and were not included in siderophile means. The ungrouped Ningqiang fall plots together with the CV chondrites. Older data by Kallemeyn and coworkers shown as stick symbols. See Table 1 for abbreviations.

Kallemeyn et al. (1991) resulted from metamorphic recrystallization and impact-induced crushing.

Amoeboid olivine inclusions (AOIs) constitute ~3.5 vol.% of oxidized CV chondrites (McSween, 1977a). These fine-grained objects are composed of major olivine, major to minor Ca-pyroxene, minor anorthite, accessory metallic Fe–Ni and perovskite. Although difficult to distinguish from recrystallized matrix in metamorphosed chondrites, AOIs were reported in CK3 NWA 1559 (Brandstätter et al., 2003; Rubin, 2013; Fig. 4), CK4 Karoonda (McSween, 1977b) and CK4-an Maralinga (Keller et al., 1992).

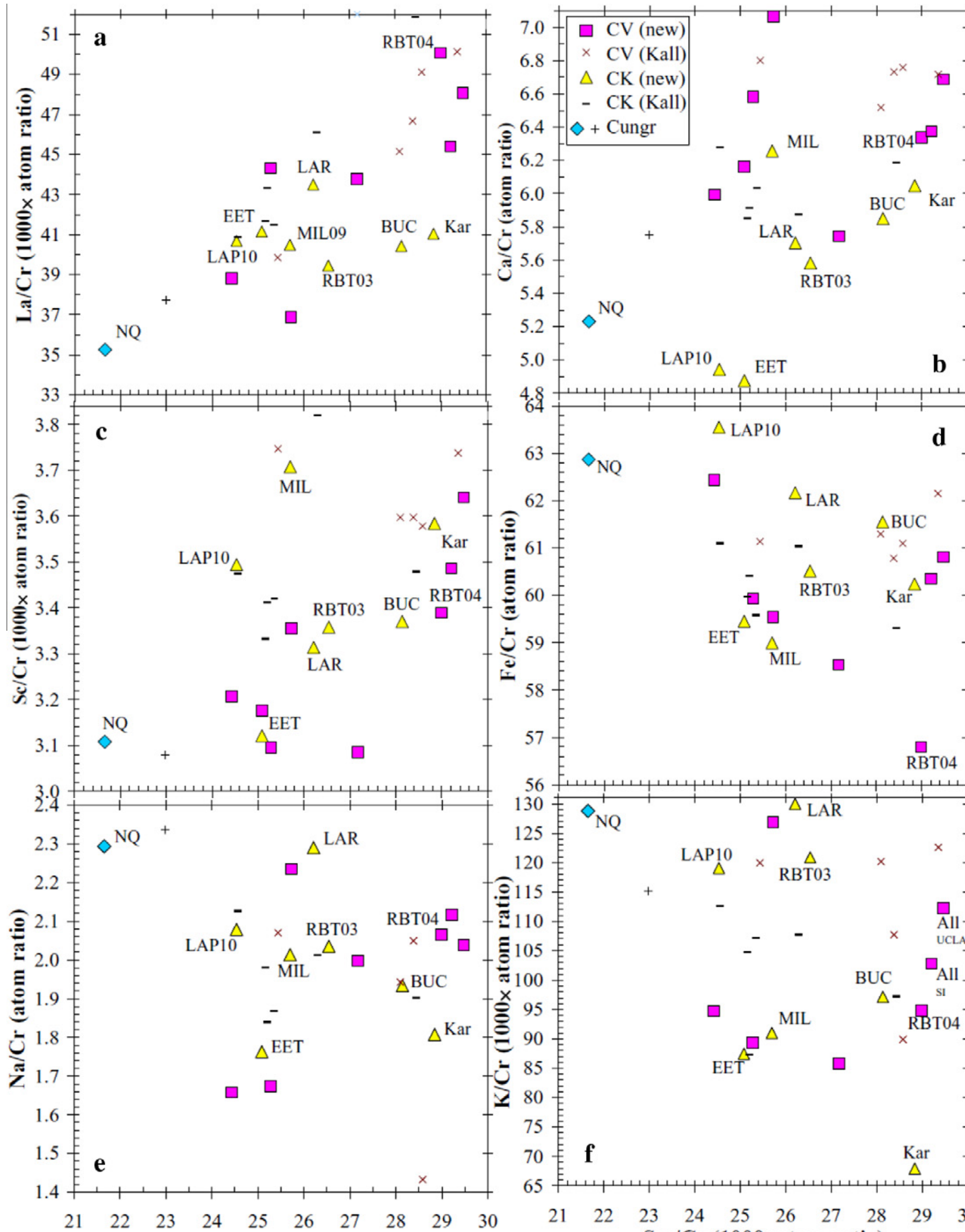

Fig. 6. Plots of Cr-normalized abundances of lithophiles against Sm. In (a–c) the abundances of refractory lithophiles La, Ca, Sc and Sm show some scatter but no systematic differences; the same conclusion is obtained for the older data by Kallemeyn and coworkers. Fe abundances (d) also show no differences between the two groups. The alkalis Na and K (e, f) scatter a bit, but show no systematic differences between CK and CV. Refractory lithophiles are ~20% low in Ningqiang; Fe, Na and K are high, similar to the highest values observed in CV and CK.

4. DISCUSSION

4.1. Application of elemental composition data

4.1.1. Are CV and CK chondrites part of the same group?

We show our results in Figs. 5–7. On each scatter diagram we plot our data as large filled symbols and the earlier data of Kallemeyn and coworkers as small stick symbols. It is important to note that the Kallemeyn et al. data were published (and gathered) over an extended period; the CV data were published in 1981, the CK data in 1991 and the Ningqiang data in 1989. Because our data generally agree with the data from Kallemeyn et al., we only discuss the latter in a few special cases. For various reasons we do not

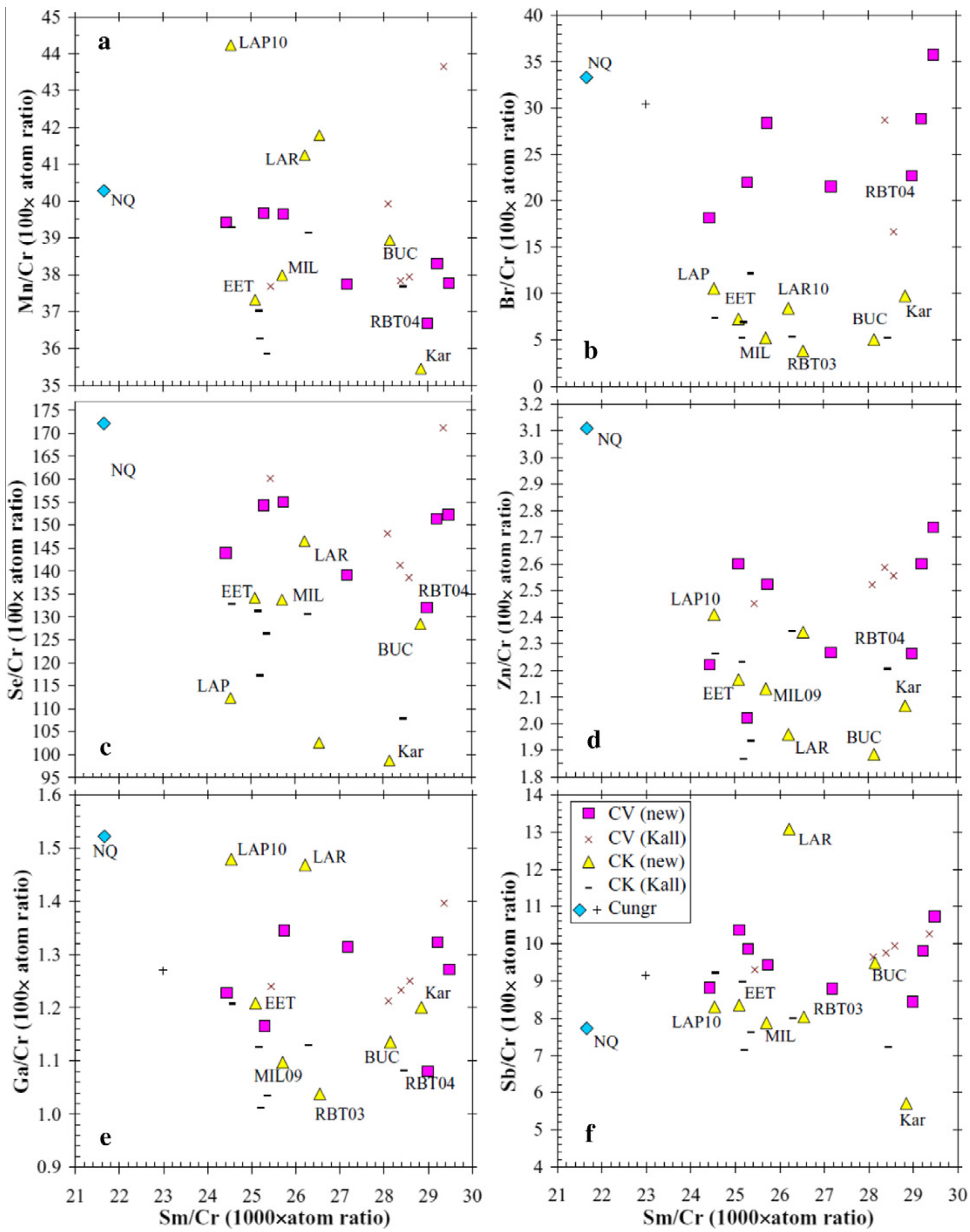

Fig. 7. Plots of Cr-normalized abundances of volatiles against Sm; most of these elements have siderophile and chalcophile affinities. The least volatile element, Mn (a) shows no resolvable difference between CV and CK. Abundances of the most volatile element Br (b) are about 4× lower in CK than in CV, evidence of major loss during the metamorphism event (likely to be of impact origin). Mean abundances of the remaining four moderately volatile elements (Se, Zn, Ga and Sb) are about 10% lower in CK than CV, but individual values overlap. See Table 1 for abbreviations.

plot the five "unfractionated" CKs from Huber et al. (2006). For two of them, LAP 03784 and LAR 04318, we analyzed a second sample and averaged these with the earlier data; these are plotted as new analyses. Two others were analyzed only once by Kallemeyn and we plan additional study. The fifth sample, NWA 765, has a Au value that we now consider too low to be called unfractionated, and has been subjected to the usual North African weathering processes.

It is useful to plot bulk compositional data as abundances, i.e., as atomic ratios of the element being considered relative to a normalizing element. In the absence of Mg and Si data we have normalized our results to Cr. We tested Mn as an alternative but concluded that Cr gave less scatter attributable to the normalizing element. In most of the following discussion we mention only the element in the numerator, not the Cr. Note that Table 1 lists the abbreviations used for the different meteorites in the figures and in the following discussion.

As noted above, some of our CK samples show siderophile/chalcophile fractionations attributable to weathering, a problem addressed in considerable detail by Huber et al. (2006). In Fig. 5 we plot the siderophiles Co, Au, Se, Ir, As and Sb against Ni; Au, Se, Co and Ni are the elements that are the most sensitive to terrestrial weathering effects. To set the stage we first discuss the CV-chondrite data for these four elements.

The ranges for our new siderophile and chalcophile CV data (filled squares) are relatively low (maximum/minimum ratios of ~1.3) for all seven elements. There is a strong correlation between Co and Ni (Fig. 5a); the data scatter near an arbitrary constant-ratio (0.050) reference line. With the exception of GRA 06101 (the low-Au CV in Fig. 5b), the Au–Ni trend is similarly clustered near a slope of 3.2×10^{-6}. There is no apparent correlation of the other four elements with Ni (Fig. 5c–f). In most cases Ningqiang plots with the CV chondrites, plotting slightly higher in Se and slightly lower in Sb.

The same elements in CK (filled triangles) show larger ranges and more scatter. A correlation with Ni is observed only for Co (Fig. 5a); the correlation included the low values in CK MIL09 and RBT03 and the very high values in LAR. If LAR is neglected, the CKs plot near the CV trend. In the Au–Ni diagram (Fig. 5b) we find a CV-like Au content for RBT03, but very low values for MIL and LAP10 and somewhat low values for LAR and BUC. In Fig. 5c we see that Se is very low in MIL, BUC and LAP10. The remaining siderophiles Ir (Fig. 5d), As (Fig. 5e) and Sb (Fig. 5f) show less pronounced weathering effects than these elements (but Sb is quite low in Karoonda). Based on the high values for Ni and Co in LAR and the low values for two or more siderophiles in RBT03, MIL, BUC and LAP10, we chose to base our CK means for siderophile and chalcophile elements (Co, Ni, Ru, Ga, As, Se, Sb, Os, Ir, Au) on only two chondrites, EET and Karoonda.

In Figs. 6 and 7 we plot lithophile/Cr ratios against Sm/Cr. Some of the elements in Fig. 7 also have siderophile and chalcophile affinities. In each diagram the newer results agree well with the earlier data by Kallemeyn and coworkers. Only in two cases did we alter the Kallemeyn et al. data to improve the agreement with the new data: we multiplied all Ir by 0.9 to bring it close to the newer data. The As corrections were more complex; we multiplied the CV data by 0.9 and the CK data (gathered 10 years later) by 1.05 to bring them into better agreement with our newer data. These factors are chosen to undercorrect; they are slightly closer to unity than our best estimate of the ratio between the two data sets.

In this paper the most relevant data are those for the refractory lithophiles. In Fig. 6a–c the refractory lithophiles La, Ca and Sc are plotted against Sm, also a refractory lithophile. There is a rough positive correlation in each diagram which is strongest for CV La–Sm (Fig. 6a). The correlation between Ca and Sm is very weak, attributable to the high degree of scatter in our CK Ca/Cr ratios (the relative standard deviation is 9.1%, much higher than that for Sm/Cr, 5.8%). The other elements plotted in Fig. 6 (Fe, Na, K) scatter a bit but show no systematic differences between CK and CV. The main conclusion that can be reached from Fig. 6 is that there is no clearly resolvable difference between CV and CK for these elements.

The elements plotted on the vertical axes in Fig. 7 are highly volatile (Br) or moderately volatile (Zn, Ga, Se, Mn). All except Mn have resolvably low CK/CV ratios but the fields overlap for all elements except Br. Scenarios that may have led to the loss of volatiles from the CK materials are discussed below. Some of these elements were affected by terrestrial weathering, with Se being the most susceptible. Because the CKs LAR and MIL09 have low Au and Ni values due to significant weathering, the low Zn in the former and the low Se and high Sc in the latter should be neglected.

In Table 4 we list the mean compositions of CK and CV chondrites based on our new data. We remind the reader that we analyzed seven members of each group, but that some meteorites were not included in the means. Among the CV chondrites, we did not include our data for RBT04 in any means; the UCLA and SI samples of standard Allende were treated as separate samples. Among the CK chondrites, two meteorites (LAR and LAP10) were excluded from lithophile means, and five meteorites (all except Karoonda and EET) were excluded from the siderophiles-and-others means. This makes the latter means especially sensitive to unrepresentative sampling.

In Fig. 8 we plot mean Cr-normalized CK/CV abundance ratios. These are separated into two traditional categories: lithophiles and siderophiles-and-others (Se, Zn and Br). Within each of these categories, the elements are ordered approximately in terms of volatility increasing to the right. Most of the "others" elements are chalcophiles. For meteorites with the high degree of oxidation currently present in CK chondrites, some of these elements (e.g., Zn, As) may now be present as oxides. However, it seems probable that, during nebular condensation, they were mainly present as metals or sulfides.

Refractory lithophile abundances are key taxonomic parameters for classifying chondrites (Kallemeyn and Wasson, 1981; Wasson and Kallemeyn, 1988). Well-determined refractory lithophile (Sc, Sm, Eu) abundances vary by a factor of 2.5 among the chondrite groups, but are generally the same within a factor of <1.2 within individual groups. The spread among the different groups is attributed to variations in a refractory-lithophile nebular component closely related to Ca–Al-rich (i.e., refractory) inclusions.

The refractory lithophile data in Fig. 8 make a strong case for CK and CV chondrites being from the same nebular formation location. As noted above, RBT04 was not included in the CV mean; CK lithophiles and Fe means are based on EET, Kar, RBT03 and BUC; CK siderophiles and others are based only on Kar and EET. For the three well-determined refractory lithophiles there is no observable difference in abundance ratios between the two groups. The observed small differences in Ca, Lu, Yb and La are attributed to analytical and sampling errors for these elements.

Table 4
Bulk compositions of relatively unweathered CK and CV chondrites and the CK/CV ratio. See text for discussion of sample choice for averaging. Ratios for moderately volatile elements are in the range 0.8–0.95, highly volatile Br is 0.26. Because Cr is 5% higher in CK relative to CV, element/Cr abundances are lower by this amount. The large Os ratio appears to reflect our relatively large errors in Os analyses.

Element	Na (mg/g)	K (μg/g)	Ca (mg/g)	Sc (μg/g)	Cr (mg/g)	Mn (mg/g)	Fe (mg/g)	Co (μg/g)	Ni (mg/g)	Zn (μg/g)	Ga (μg/g)	As (μg/g)
CK	3.00	251	15.5	10.5	3.61	1.46	234	664	13.5	97	5.55	1.25
CV	3.00	265	17.0	9.9	3.46	1.41	224	653	13.0	105	5.9	1.50
CK/CV	1.00	0.95	0.91	1.06	1.04	1.03	1.05	1.02	1.03	0.92	0.94	0.83
Element	Se (μg/g)	Br (μg/g)	Ru (μg/g)	Sb (ng/g)	La (ng/g)	Sm (ng/g)	Eu (ng/g)	Yb (ng/g)	Lu (ng/g)	Os (ng/g)	Ir (ng/g)	Au (ng/g)
CK	7.40	0.36	1.12	61	423	283	114	306	44	989	779	150
CV	7.8	1.4	1.04	78	429	269	107	312	44	723	673	140
CK/CV	0.94	0.26	1.07	0.79	0.99	1.05	1.06	0.98	1.00	1.35	1.16	1.07

At the right end of the lithophiles in Fig. 8, the slightly volatile Mn is the same in CK and CV, but Na and K are slightly lower in CK, perhaps reflecting volatilization loss as discussed below.

The siderophiles-and-others category is also generally consistent with CK and CV chondrites having formed in the same part of the nebula, but there are exceptions. We attribute the differences between CK and CV in Os and Ir mainly to sampling error although, Os is also one for which we have relatively low precision. These elements are high in four of the five replicates for the two chondrites (Kar and EET) whose data are averaged. Because of the severe weathering effects present even in relatively unweathered Antarctic finds, we hold it to be possible that fractionations have played a role, perhaps even on a scale of millimeters, during aqueous alteration on the CK asteroid.

The next five siderophiles (Ru, Ni, Co, Fe, Au) have abundance ratios near unity, consistent with CK and CV chondrites forming from the same nebular materials. The following six elements all have resolvably low CK/CV ratios and there is little doubt that this reflects volatility. The first five (As, Sb, Ga, Se, Zn) have abundance ratios in the range 0.9–0.8 within experimental uncertainties and fall together with Na and K into the category of moderately volatile elements. In contrast, Br has a much lower ratio of 0.26. According to Fegley and Lewis (1980) Br has a very low 50% condensation temperature of 380 K; it appears that, like the element In in OC (categorized as highly volatile by Tandon and Wasson, 1968), its behavior is qualitatively different. A volatile loss scenario is discussed below.

Our current interpretation is that these data do not support the conclusion of Kallemeyn et al. (1991) that there are inherent compositional differences in CK and CV that were established in the solar nebula. We conclude that the best working model is that CK chondrites are metamorphosed (and otherwise altered) CV chondrites.

4.1.2. Relationship of Ningqiang to CV/CK chondrites

Ningqiang was classified as CV3-an by Rubin et al. (1988), categorized as $CV3_{OxA}$ by Weisberg and Prinz (1998), and reclassified as CK3-an by Kallemeyn et al. (1991). Our compositional data support earlier studies that showed Ningqiang to have higher Zn than normal CK or CV. Our Ningqiang sample records low abundances of the three best-determined refractory lithophile elements (Sm, La and Sc) (Fig. 6) although a few CV and CK chondrites have similarly low Sc. The La and Sm values of Rubin et al. (1988) (plotted as a plus) are also low, but closer to CV and CK values than are the newer values. These lower-than-CV refractory lithophile data open the possibility that Ningqiang might not be a member of the CV/CK set of chondrites. It seems best to follow the Kallemeyn (1996) characterization of Ningqiang as an ungrouped carbonaceous chondrite.

4.1.3. Reclassification of MIL 090001 as a CR2 chondrite

Keller (2011) designated MIL 090001 a CV2, the CV assignment based on a preliminary classification; this would have made it only the second CV chondrite (after Mundrabilla 012; Ulff-Møller et al., 1993) described as showing

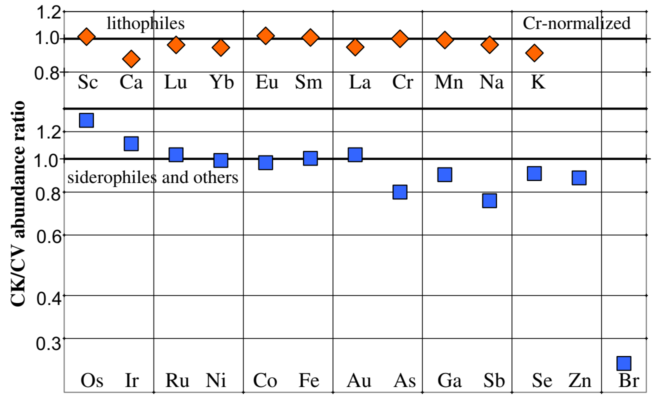

Fig. 8. Plot of mean Cr-normalized CK/CV abundance ratios, separated into two traditional categories: lithophiles (upper row) and siderophiles-and-others (lower row). Within each of these categories, the elements are ordered approximately in terms of increasing volatility to the right. As discussed in the text, CV abundances are based on six chondrites, CK lithophile abundances on four chondrites, and siderophile-and-other-element abundances based on Kar and EET. See text for details. The CK Os enhancement probably reflects experimental error and impact-induced sampling heterogeneities. The CK volatile depletions are attributed to the process (probably impacts) that produced the thermal metamorphic recrystallization in the CKs.

the high degree of alteration associated with petrographic type 2. The large size of the chondrules in MIL 090001 is consistent with it being a CV chondrite, but would also be consistent with a CR-chondrite designation.

In Table 5 we compare our INAA data for MIL 090001 with our CV data from Table 4 and with the CR data from Kallemeyn et al. (1994); in terms of refractory lithophiles, MIL 090001 much more closely resembles the CR composition. MIL 090001 has some compositional features that are different from both groups. In particular, it has very low Na and low K and Fe contents; these might reflect impact-induced fractionations on the asteroid or weathering effects on Earth. Some differences with CR, such as its lower Os and Ir contents, could reflect biases between the two data sets.

The whole-rock O-isotopic composition of MIL 090001 (Keller et al., 2012) plots on the CR-chondrite mixing line (Schrader et al., 2011), consistent with its reclassification by Isa et al. (2012) and Keller et al. (2012) as a CR2. Observations by Harju et al. (submitted for publication) show it to be approximately as aqueously altered as CR2.4 Renazzo.

4.1.4. Comparison with published data

In the above discussion we compare our CV data with those published by Kallemeyn and Wasson (1981) and our CK data with those of Kallemeyn et al. (1991). With the exception of systematic errors discussed above for Ir and As, the agreement between the data sets is very good.

Greenwood et al. (2010) determined 16 elements in CK and CV chondrites by ICP-MS; their Al/Mg, Ca/Mg and Sc/Mg fields for CK and CV overlapped. All their CK chondrites except Karoonda (a fall) were collected from hot deserts and a large fraction show weathering effects. Their sample sizes were small (6–20 mg splits of larger, homogenized samples). Our data are in general agreement with theirs (to within about 5%), but there are some systematic differences (e.g., their Sc values are about 1.1 × higher).

In the abstract by Isa et al. (2011) there are diagrams showing abundance data for 30 elements in 19 Antarctic CK chondrites and about four CV chondrites using INAA and ICP-MS, the latter mainly to determine highly volatile elements Cd, Tl, Pb and Bi. No numerical data are tabulated; thus, we cannot make a detailed comparison with our values.

4.2. Transforming CV into CK

The most primitive of the $CV3_R$ meteorites best preserve the record of materials that formed in the solar nebula, although Hurt et al. (2012) showed that the fine matrix in their section of $CV3_R$ Vigarano exhibits extensive alteration, and many samples of Vigarano have undergone appreciable terrestrial weathering (e.g., Abreu and Brearley, 2005). It seems likely that the two oxidized CV subgroups ($CV3_{OxA}$ and $CV3_{OxB}$) as well as the CK chondrites formed by oxidation caused by chemical/textural alteration of primitive $CV3_R$ materials. In fact, Brearley (2009) found that matrix olivine grains in NWA 1628 (CK~3.8) are coarser than those in $CV3_{OxA}$ Allende, but otherwise resemble them in morphology and microstructure. There is general agreement within the cosmochemical community that H_2O was the main oxidizing agent for chondritic materials (e.g., Meeker et al., 1983; Greenwood et al., 1994; Choi et al., 1998; Krot et al., 1998a,b; Sakamoto et al., 2007). We assume that this holds also for the CV–CK chondrites.

An interesting question is whether $CV3_{OxA}$, $CV3_{OxB}$ and CK chondrites represent different stages in a single line of descent or whether they each followed individual oxidation/alteration paths. For convenience we will use the latter as our starting assumption (because this temporarily permits us to neglect the evidence recorded in $CV3_{OxA}$ and $CV3_{OxB}$ samples), but we will later examine the possibility that the single-line-of-descent scenario is more attractive.

Table 5
Comparison of the mean composition of MIL 090001 with the Kallemeyn et al. (1994) composition of CR2 and the CV3 chondrite mean from Table 4. Within the scatter in the MIL 090001 data there is good agreement with the exception of low Na, K and Fe in MIL 090001.

Element	Na (mg/g)	K (µg/g)	Ca (mg/g)	Sc (µg/g)	Cr (mg/g)	Mn (mg/g)	Fe (mg/g)	Co (µg/g)	Ni (mg/g)	Zn (µg/g)	Ga (µg/g)	As (µg/g)
CR2	3.23	303	13.8	8.5	3.75	1.70	240	667	13.6	70	4.6	1.40
MIL 090001	0.97	200	13.5	7.5	3.46	1.82	214	682	12.0	61	4.8	1.50
CV3	3.00	265	17.0	9.9	3.46	1.41	224	653	13.0	105	5.9	1.50
Element	Se (µg/g)	Br (µg/g)	Ru (µg/g)	Sb (ng/g)	La (ng/g)	Sm (ng/g)	Eu (ng/g)	Yb (ng/g)	Lu (ng/g)	Os (ng/g)	Ir (ng/g)	Au (ng/g)
CR2	5.2	1.2	0.94	61	342	210	84	236	35	679	642	139
MIL 090001	6.6	0.8	0.92	47	291	187	84	231	35	582	539	162
CV3	7.8	1.4	1.04	78	429	269	107	312	44	723	673	140

CK chondrites are more metamorphosed than the $CV3_{OxA}$ and $CV3_{OxB}$ subgroups. Although recent models of the CV parent body based on magnetic studies have suggested that the parent asteroid may have had a molten core (e.g., Weiss et al., 2010; Carporzen et al., 2011; Elkins-Tanton et al., 2011), this view was challenged by Bland et al. (2011) who attributed the magnetic properties of CV materials to impacts. We agree with this latter view and have discussed in previous papers that metamorphic reheating seems to be associated with impacts (e.g., Rubin, 1995, 2004).

Although we cannot rule out minor heating by ^{26}Al, there is strong evidence for impact and shock features in the CK chondrites: (a) fractures were formed in the silicate grains (e.g., Fig. 3d), (b) opaque phases were melted and injected into some of these fractures, causing silicate darkening (Fig. 3 of Rubin, 1992), (c) silicate-rich shock veins were formed (Fig. 1 of Rubin, 1992), and (d) some of the plagioclase was melted, partly volatilized, mobilized, and recrystallized into grains with variable compositions (Table 1 of Rubin, 1992). In our opinion, the weight of the evidence favors impact heating and we will not attempt to examine radiogenic heating (e.g., McSween et al., 2002) or solar heating at a perihelion <0.2 AU (Chaumard et al., 2012) as viable alternatives.

Among those CK chondrites that exhibit extensive crushing, the average size of clastic grains increases from ~11 µm in CK3.8 NWA 1559 (Fig. 2a) to ~20 µm in CK4 Karoonda (Fig. 2b), ~35 µm in CK4 NWA 5025 (Fig. 2c) and ~50–60 µm in CK5 LAP 10030 (Fig. 2f). The larger grain size and the evidence that metamorphism destroyed shard-like surfaces of CK chondrites of higher petrologic type suggest that these rocks experienced metamorphic recrystallization after the impact-induced crushing event. It is probably not a coincidence that most of the CK chondrites are extensively oxidized, crushed and nearly or completely equilibrated. We suggest that the high-degree of crushing of CK precursor materials increased the specific surface area and led to enhanced susceptibility to thermal alteration and recrystallization.

All of the CV3 chondrites probably started off as reduced rocks akin to Vigarano, Arch, Efremovka and Leoville; their initial abundance of metallic iron is not clear but data reported by McSween (1977a) suggest that it was in the range of 40–80 mg/g. We estimate that the metallic Fe–Ni content of CK chondrites is <1 mg/g.

During parent-body aqueous alteration of $CV3_R$ chondrites, metallic Fe is partly converted to Fe^{3+} which is largely incorporated into magnetite. In $CV3_{oxB}$ samples the fraction of Fe^{3+} seems to decrease as a result of Fe from metal and magnetite being converted into Ca–Fe-rich silicates (hedenbergite and andradite) and fayalite; phyllosilicates also form (e.g., Krot et al., 1998a,b, 2005). $CV3_{oxA}$ chondrites have less-ferroan olivine and only rare phyllosilicates; they appear to be less altered than $CV3_{oxB}$ materials.

As pointed out by Greenwood et al. (2010), it is unlikely that CK chondrites descended from $CV3_{oxB}$ rocks. The experiments of Mayeda and Clayton (1998) suggest that thermal dehydration of a phyllosilicate-rich rock would produce a rock with heavier O isotopes. This is contrary to the case of CK chondrites which have lighter O isotopes than $CV3_{oxB}$ chondrites (e.g., Fig. 8 of Greenwood et al., 2010). However, we have not been able to infer whether CK chondrites descended from $CV3_{oxA}$ rocks or followed an independent oxidation path from reduced $CV3_R$ materials.

If CK4–6 chondrites are actually metamorphosed CV3 chondrites, the question arises as to where CK3 samples fit into this sequence. Essentially all classified CK3 chondrites appear to be appreciably metamorphosed with Fa30 olivine. For example, NWA 1559 is extensively recrystallized and is likely to be subtype 3.8 (Rubin, 2013). Similarly, the Meteoritical Bulletin online database lists NWA 2921 as CK3.8 and NWA 2854 as CK3/4; Chaumard et al. (2009) list NWA 4724 (CK3.8), NWA 4425 (CK3.8) and NWA 4423 (CK3.9); Brearley (2009) describes NWA 1628 as being "high petrologic type 3", presumably ~3.8. The CK3.8, CK3.9 and CK3/4 chondrites have very ferroan olivine-rim compositions (typically around Fa 30) with little grain-to-grain compositional variation. The presence of moderately equilibrated olivine with Fa~30 provides the key parameter indicating CK-group membership. It is plausible that (a) most or all of the CK3 chondrites are of relatively high petrologic subtype ($\geqslant$3.8) and have uniformly high olivine Fa contents (which is why they are designated CK in the first place), and (b) CV–CK-like samples that are less equilibrated and have lower mean olivine Fa contents (e.g., MET 01017; Busemann et al., 2007; Alexander et al., 2007) are routinely classified as CV3. It appears that investigators routinely assigned unequilibrated metal-poor, magnetite-bearing rocks with large chondrules to the CV group and equilibrated rocks with these same petrographic characteristics to the CK group.

4.3. Fractionation processes and the relationship between CV and CK groups

4.3.1. Fractionations associated with weathering

As discussed in Kallemeyn et al. (1991) and Huber et al. (2006), the weathering fractionations in CK chondrites appear to reflect dissolution and transport that occurred following the wetting of the samples by rains. Huber et al. (2006) inferred that it was Ni-rich sulfides such as pentlandite and pyrrhotite that were particularly vulnerable. After the dissolution of hygroscopic minerals the siderophile behavior seems to have been largely controlled by electrochemistry. Elements that are easily reduced such as Ir tended to stay close to the location where their parental phase dissolved. Others that remained oxidized moved farther and thus were more likely to escape the meteorite. However, some of these may have been reduced again within the meteorite, leading to enhanced concentrations (e.g., Os and Ir in Karoonda).

4.3.2. Volatile-element fractionations

It was noted above that moderately volatile elements are lower in CK than in CV. With the exception of Mn and Na, CK values are 0.91 to 0.75 × those in CV chondrites.

The most interesting element is Br with a CK abundance in our two "unweathered" samples (CK4 Karoonda and CK5 EET) that is 4× lower than the CV mean. The Br contents in the weathered samples are similarly low.

Isa et al. (2011) obtained ICP-MS data for several highly volatile elements in CK and CV chondrites. Their mean Bi values in CK are ~3× lower than in CV and their mean Tl values are ~30× lower than CK values, but In, which strongly decreases with increasing petrographic type in ordinary chondrites (Tandon and Wasson, 1968; Keays et al., 1971), showed no resolvable variation between CK and CV. Isa et al. observed no systematic variation in Bi and Tl with petrographic type. They concluded that the CK volatile patterns were established by nebular processes rather than by asteroid metamorphism and averred that CKs and CVs had different nebular origins and should be treated as separate groups.

If, contrary to the conclusion of Isa et al. (2011), we maintain that CK chondrites are metamorphosed CV materials, we need to explain the much lower Br (and Bi and Tl) contents in CK. Although it has been common practice to attribute such differences to thermal metamorphism, it is not easy to lose trace volatiles during thermal metamorphism of an internally heated body (i.e., one heated by the decay of ^{26}Al). The problem is that volatiles that evolved deep within an asteroid would condense again when they migrated to a cooler part of the body nearer the surface. There will thus be no loss from the asteroid, only a redistribution. This leads to the prediction that volatiles will show different distributions based on their relative volatilities; the more volatile the element, the higher in the body its peak abundance will be located.

In L chondrites, Tandon and Wasson (1968) found a strong correlation between the In concentration (with a total range of a factor of 1000) and petrographic type. Similar (although less well-correlated) ranges are also observed for Ar (Zähringer, 1966), Kr (Marti, 1967) and Br, Cs, Bi and Tl (Keays et al., 1971).

Wasson (2005) noted the problems with losing volatiles from asteroids with internal heat sources, and suggested that impact heating was responsible for volatile loss. As noted above, there is much evidence that metamorphic heating of asteroids is largely the result of impacts (e.g., Rubin, 1995, 2004). Our scenario is that, in the nebula, the highly volatile elements condensed onto particle surfaces at low temperatures, and that these volatiles partly flashed off during impacts very early in the history of the asteroid. This not only selectively vaporized these surface-correlated volatiles and their host phases (probably mainly amorphous materials in the fine fraction), it also created a hot carrier gas consisting of H_2O, H_2S and carbon-bearing gases such as CH_4 and CO. The highly volatile elements were entrained with these gases as they escaped.

CK chondrites resemble L and LL chondrites in having no correlation between depletions in moderately volatile elements and petrologic type. There is little published data for highly volatile elements in CK chondrites, but in L and LL chondrites these elements do show an anticorrelation with petrologic type. We suggest that the apparent differences between CK and L-and-LL chondrites in the behavior of moderately and highly volatile elements are associated with differences in the whole-rock composition and properties of the two kinds of materials. At the L/LL chondrite formation location, the nebular materials were more oxidized (i.e., there was a much larger fraction of high-FeO chondrules) and that may have resulted in a different set of elements being incorporated onto grain surfaces or into amorphous grains.

Another possible difference is in oxidation/heating scenarios. In general, such oxidation events are plausibly attributed to hydrothermal processes. If, in CK chondrites, the oxidation had already occurred before the volatilization event, highly volatile elements that were on surfaces in nebular materials may have been redistributed; some may have been concentrated in new phases that did not experience extensive loss during flash volatilization.

5. CONCLUSIONS

On the basis of new duplicate INAA data for seven CV and seven CK chondrites we conclude that the two groups cannot be resolved in terms of refractory and common lithophile elements. Based on this evidence we agree with Greenwood et al. (2010) that the two groups should be merged. We recommend that the "CK" designation be abandoned and that the range of petrologic types encompassed by the CV group be extended from 3 to 6. It seems likely that CK chondrites formed from reduced CV3 materials as a result of heating and fragmentation by impacts. Oxidation by H_2O, loss of volatiles, and recrystallization transformed CV chondrites into CK chondrites. Because it is unclear which CV3 subgroup served as the immediate precursor of CK chondrites, we recommend that CK3 chondrites be designated $CV3_{OxK}$.

Volatile-element abundances in CK chondrites are lower than those in CV chondrites; moderately volatile elements are 10–20% lower in CK and the highly volatile element Br is about 4× lower in CK relative to CV. This behavior of highly volatile elements is similar to that observed in ordinary chondrites. Tandon and Wasson (1968) found variations of a factor of 1000 in In contents among L chondrites that correlated with petrographic type, but no correlation with type is observed among the CK chondrites. Because some CK chondrites apparently were shocked and heated more than once (e.g., Rubin, 1992), this could have led to the redistribution of some volatiles, causing diminishment in the correlation between volatile concentrations and metamorphic recrystallization effects.

Kallemeyn et al. (1991) concluded that the CK- and CV-chondrite groups had distinct origins because the two groups were fully resolved by Al/Mg ratios. However, they reported a total maximum/minimum range of only 1.06 in CK chondrites; the scatter in the other well-determined refractory lithophiles Sc and Sm is appreciably larger, 10% and 13%, respectively. We suspect that the Al values were fortuitously low; with the higher and more typical amount of scatter, there would probably have been appreciable overlap of the CV and CK data.

Our elemental abundance data imply that the best working model is that the CV and CK chondrites are samples processed from the same nebular materials. And as noted by Greenwood et al. (2010), the similarity in cosmic-ray exposure-age distributions among members of these groups supports the view that they originated in the same asteroidal parent.

Kallemeyn et al. (1991) stated that there are significant textural differences between CK and CV chondrites aside from the fact that CK samples are more metamorphosed; these differences include the apparently low abundances in CK chondrites of CAIs and chondrules with igneous rims. Our new observations show that these features are present in CK chondrites in abundances similar to those in CV. Our new observations on a larger set of thin sections show that most CK chondrites have experienced extensive crushing prior to metamorphism; this led to a major increase in the surface areas of mineral grains, thereby enhancing the rate of recrystallization. It also facilitated oxidation via aqueous alteration. It appears that the low apparent modal abundances in CK chondrites of CAIs and chondrules with igneous rims are solely attributable to the shock, thermal and parent-body alteration histories of the CK samples.

ACKNOWLEDGMENTS

We thank Frank Kyte for technical assistance. We are indebted to Richard Greenwood, Makoto Kimura, and Associate Editor Sara Russell for helpful reviews. This research was mainly supported by NASA Grants NNG06GG35G and NNX10AG98G (J.T.W.) and NNG06GF95G (A.E.R.).

APPENDIX A. SUPPLEMENTARY DATA

Supplementary data associated with this article can be found, in the online version, at http://dx.doi.org/10.1016/j.gca.2013.01.011.

REFERENCES

Abreu N. M. and Brearley A. J. (2005) Carbonates in Vigarano: Terrestrial, preterrestrial, or both? *Meteorit. Planet. Sci.* **40**, 609–625.

Alexander C. M. O'D., Fogel M., Yabuta H. and Cody G. D. (2007) The origin and evolution of chondrites recorded in the elemental and isotopic compositions of their macromolecular organic matter. *Geochim. Cosmochim. Acta* **71**, 4380–4403.

Bland P. A., Muxworthy A. R., Collins G. S., Moore J., Davison T. M. and Ciesla F. J. (2011) Heterogeneous shock in porous chondrites: implications for Allende magnetization (abstract#5275). *Meteorit. Planet. Sci.* **46**, A22.

Brandstätter F., Bukovanská M. and Kurat G. (2003) NWA 1559: another anomalous CK3 chondrite (abstract). *Meteorit. Planet. Sci.* **38**, A63.

Brearley A. J. (2009) Matrix olivines in the metamorphosed CK chondrite NWA 1628: possible affinities to olivines in the matrices of oxidized CV3 chondrites and dark inclusions (abstract). *Lunar Planet. Sci.* **40**, 1791, pdf.

Bukovanská M., Brandstätter F. and Kurat G. (2003) NWA 1560 (CK4/5) and NWA 1565 (CK5) – a comparison with HaH 280 (CK4) chondrite (abstract). *Meteorit. Planet. Sci.* **38**, A84.

Busemann H., Alexander C. M. O'D. and Nittler L. R. (2007) Characterization of insoluble organic matter in primitive meteorites by microRaman spectroscopy. *Meteorit. Planet. Sci.* **42**, 1387–1416.

Cain P., McSween H. Y. and Woodward N. B. (1986) Structural deformation of the Leoville chondrite. *Earth Planet. Sci. Lett.* **77**, 165–175.

Carporzen L., Weiss B. P., Elkins-Tanton L. T., Shuster D. L., Ebel D. and Gattacceca J. (2011) Magnetic evidence for a partially differentiated carbonaceous chondrite parent body. *Proc. Natl. Acad. Sci. USA* **108**, 6386–6389.

Chaumard N., Devouard B., Zanda B. and Ferrière L. (2009) The link between CV and CK carbonaceous chondrites based on parent body processes (abstract). *Meteorit. Planet. Sci.* **44**, A49.

Chaumard N., Devouard B., Zanda B. and Devidal J.-L. (2011) Metamorphosed calcium–aluminum-rich inclusions in the Tanezrouft 057 CK4 carbonaceous chondrite (abstract). *Lunar Planet. Sci.* **42**, 1924, pdf.

Chaumard N., Devouard B., Delbo M., Provost A. and Zanda B. (2012) Radiative heating of carbonaceous near-Earth objects as a cause of thermal metamorphism for CK chondrites. *Icarus* **220**, 65–73.

Choe W. H., Huber H., Rubin A. E., Kallemeyn G. W. and Wasson J. T. (2010) Compositions and taxonomy of 15 unusual carbonaceous chondrites. *Meteorit. Planet. Sci.* **45**, 531–554.

Choi B.-G., McKeegan K. D., Krot A. N. and Wasson J. T. (1998) Extreme oxygen-isotope compositions in magnetite from unequilibrated ordinary chondrites. *Nature* **392**, 577–579.

Elkins-Tanton L. T., Weiss B. P. and Zuber M. T. (2011) Chondrites as samples of differentiated planetesimals. *Earth Planet. Sci. Lett.* **305**, 1–10.

Fegley B. and Lewis J. S. (1980) Volatile element chemistry in the solar nebula: Na, K, F, Cl, Br, and P. *Icarus* **41**, 439–455.

Geiger T. and Bischoff A. (1995) Formation of opaque minerals in CK chondrites. *Planet. Space Sci.* **43**, 485–498.

Geiger T., Spettel B., Clayton R. N., Mayeda T. K. and Bischoff A. (1993) Watson 002 – the first CK type-3 chondrite (abstract). *Meteoritics* **28**, 352.

Greenwood J. P., Wasson J. T. and McKeegan K. D. (2000a) Metamorphosed CAI in Karoonda: constraints on CK metamorphism from oxygen isotopic compositions (abstract). *Lunar Planet. Sci.* **31**, 2042, pdf.

Greenwood J. P., McKeegan K. D. and Wasson J. T. (2000b) A Karoonda conundrum: primordial oxygen in magnetite, olivine and iron-rich spinel in a metamorphosed calcium–aluminum-rich inclusion (abstract). *Meteorit. Planet. Sci.* **35**, A63.

Greenwood R. C., Lee M. R., Hutchison R. and Barber D. J. (1994) Formation and alteration of CAIs in Cold Bokkeveld (CM2). *Geochim. Cosmochim. Acta* **58**, 1913–1935.

Greenwood R. C., Franchi I. A., Kearsley A. T. and Alard O. (2010) The relationship between CK and CV chondrites. *Geochim. Cosmochim. Acta* **74**, 1684–1705.

Hezel D. C., Russell S. A., Ross A. J. and Kearsley A. T. (2008) Modal abundances of CAIs: implications for bulk chondrite element abundances and fractionations. *Meteorit. Planet. Sci.* **43**, 1879–1894.

Huber H., Rubin A. E., Kallemeyn G. W. and Wasson J. T. (2006) Siderophile-element anomalies in CK carbonaceous chondrites: implications for parent-body aqueous alteration and terrestrial weathering of sulfides. *Geochim. Cosmochim. Acta* **70**, 4019–4037.

Hurt S. M., Rubin A. E. and Wasson J. T. (2012) Fractionated matrix composition in CV3 Vigarano and alteration processes on the CV parent asteroid. *Meteorit. Planet. Sci.* **47**, 1035–1048.

Isa J., Rubin A. E. and Wasson J. T. (2012) Bulk compositions of CV and CK chondrites: support for a close relationship (abstract). *Lunar Planet. Sci.* **43**, 2809, pdf.

Isa M., Shirai N., Ebihara M., Kubuki S. and Yamaguchi A. (2011) Chemical characteristics for CK carbonaceous chondrite (abstract). *Lunar Planet. Sci*. **42**, 1876 pdf.

Ivanova M. A., Nazarov A., Kononkova N. N., Taylor L. A., Patchen A., Clayton R. N. and Mayeda T. K. (2000) Dhofar 015, a new CK3 chondrite: a record of nebular processes (abstract). *Meteorit. Planet. Sci.* **35**, A83.

Kallemeyn G. W. (1996) The classificational wanderings of the Ningqiang chondrite (abstract). *Lunar Planet. Sci.* **27**, 635–636.

Kallemeyn G. W. and Wasson J. T. (1981) The compositional classification of chondrites–I. The carbonaceous chondrite groups. *Geochim. Cosmochim. Acta* **45**, 1217–1230.

Kallemeyn G. W. and Wasson J. T. (1982) The compositional classification of chondrites–III. Ungrouped carbonaceous chondrites. *Geochim. Cosmochim. Acta* **46**, 2217–2228.

Kallemeyn G. W., Rubin A. E. and Wasson J. T. (1991) The compositional classification of chondrites: V. The Karoonda (CK) group of carbonaceous chondrites. *Geochim. Cosmochim. Acta* **55**, 881–892.

Kallemeyn G. W., Rubin A. E. and Wasson J. T. (1994) The compositional classification of chondrites: VI. The CR carbonaceous chondrite group. *Geochim. Cosmochim. Acta* **58**, 2873–2888.

Keays R. R., Ganapathy R. and Anders E. (1971) Chemical fractionations in meteorites–IV. Abundances of fourteen trace elements in L-chondrites; implications for cosmothermometry. *Geochim. Cosmochim. Acta* **35**, 337–363.

Keller L. P. (1992) Petrography and mineral chemistry of calcium and aluminum-rich inclusions in the Maralinga CK4 chondrite (abstract). *Lunar Planet. Sci.* **23**, 671–672.

Keller L. P. (2011) Mineralogy and petrography of MIL 090001, a highly altered CV chondrite from the reduced sub-group (abstract). *Lunar Planet. Sci*. **42**, 2049 pdf.

Keller L. P., Clark J. C., Lewis C. F. and Moore C. B. (1992) Maralinga, a metamorphosed carbonaceous chondrite found in Australia. *Meteoritics* **27**, 87–91.

Keller L. P., McKeegan K. D. and Sharp Z. D. (2012) The oxygen isotopic composition of MIL 090001: a CR2 chondrite with abundant refractory inclusions (abstract). *Lunar Planet. Sci*. **43**, 2065 pdf.

Kracher A., Keil K., Kallemeyn G. W., Wasson J. T., Clayton R. N. and Huss G. I. (1985) The Leoville (CV3) accretionary breccia. *Proc. Lunar Planet. Sci. Conf.* **16**, D123–D135.

Krot A. N., Petaev M. I., Scott E. R. D., Choi B.-G., Zolensky M. E. and Keil K. (1998a) Progressive alteration in CV3 chondrites: more evidence for asteroidal alteration. *Meteorit. Planet. Sci.* **33**, 1065–1085.

Krot A. N., Petaev M. I., Zolensky M. E., Keil K., Scott E. R. D. and Nakamura K. (1998b) Secondary calcium-iron-rich minerals in the Bali-like and Allende-like oxidized CV3 chondrites and Allende dark inclusions. *Meteorit. Planet. Sci.* **33**, 1065–1085.

Krot A. N., Meibom A. and Keil K. (2000) A clast of Bali-like oxidized CV material in the reduced CV chondrite breccia Vigarano. *Meteorit. Planet. Sci.* **35**, 817–825.

Krot A. N., Keil K., Goodrich C. A., Scott E. R. D. and Weisberg M. K. (2005) Classification of meteorites. In *Meteorites, Comets, and Planets* (ed. A. M. Davis). Elsevier, Amsterdam, pp. 83–129.

Kurat G., Zinner E. and Brandstätter F. (2002) A plagioclase–olivine–spinel–magnetite inclusion from Maralinga (CK): evidence for sequential condensation and solid–gas exchange. *Geochim. Cosmochim. Acta* **66**, 2959–2979.

Lauretta D. S. and Killgore M. (2005) *A Color Atlas of Meteorites in Thin Section*. Golden Retriever Publications, Tucson, 301 pp.

MacPherson G. J. and Delaney J. S. (1985) A fassaite-two olivine–pleonaste-bearing refractory inclusion from Karoonda (abstract). *Lunar Planet. Sci.* **16**, 515–516.

Marti K. (1967) Isotopic composition of trapped krypton and xenon in chondrites. *Earth Planet. Sci. Lett.* **3**, 243–248.

Martin P. M., Mills A. A. and Walker E. (1975) Preferential orientation in four C3 chondritic meteorites. *Nature* **257**, 37–38.

Mayeda T. K. and Clayton R. N. (1998) Oxygen isotope effects in serpentine dehydration. *Lunar Planet. Sci*. **29**, #1405 (abstr.).

McSween H. Y. (1977a) Petrographic variations among carbonaceous chondrites of the Vigarano type. *Geochim. Cosmochim. Acta* **41**, 1777–1790.

McSween H. Y. (1977b) Carbonaceous chondrites of the Ornans type: a metamorphic sequence. *Geochim. Cosmochim. Acta* **41**, 477–491.

McSween H. Y., Ghosh A., Grimm R. E., Wilson L. and Young E. D. (2002) Thermal evolution models of asteroids. In *Asteroids III* (eds. W. F. Bottke, P. Paolicchi and R. P. Binzel). University of Arizona Press, Tucson, pp. 559–571.

Meeker G. P., Wasserburg G. J. and Armstrong J. T. (1983) Replacement textures in CAI and implications regarding planetary metamorphism. *Geochim. Cosmochim. Acta* **47**, 707–721.

Müller W. F. and Wlotzka F. (1982) Mineralogical study of the Leoville meteorite (CV3): macroscopic texture and transmission electron microscopic observations (abstract). *Lunar Planet. Sci.* **13**, 558–559.

Neff K. E. and Righter K. (2006) Opaque assemblages in CK and CV carbonaceous chondrites (abstract). *Lunar Planet. Sci*. **37**. 1320 pdf.

Noguchi T. (1993) Petrology and mineralogy of CK chondrites: implications for the metamorphism of the CK chondrite parent body. *Proc. NIPR Symp. Antarct. Meteorites* **6**, 204–233.

Norton O. R. (2002) *The Cambridge Encyclopedia of Meteorites*. Cambridge University Press, Cambridge, 354 pp.

Rubin A. E. (1984) Coarse-grained chondrule rims in type 3 chondrites. *Geochim. Cosmochim. Acta* **48**, 1779–1789.

Rubin A. E. (1992) A shock-metamorphic model for silicate darkening and compositionally variable plagioclase in CK and ordinary chondrites. *Geochim. Cosmochim. Acta* **56**, 1705–1714.

Rubin A. E. (1993) Magnetite-sulfide chondrules and nodules in CK carbonaceous chondrites: implications for the timing of CK oxidation. *Meteoritics* **28**, 130–135.

Rubin A. E. (1995) Petrologic evidence for collisional heating of chondritic asteroids. *Icarus* **113**, 156–167.

Rubin A. E. (2004) Post-shock annealing and post-annealing shock in equilibrated ordinary chondrites: implications for the thermal and shock histories of chondritic asteroids. *Geochim. Cosmochim. Acta* **68**, 673–689.

Rubin A. E. (2010) Physical properties of chondrules in different chondrite groups: implications for multiple melting events in dusty environments. *Geochim. Cosmochim. Acta* **74**, 4807–4828.

Rubin A. E. (2011) Origin of the differences in refractory-lithophile-element abundances among chondrite groups. *Icarus* **213**, 547–558.

Rubin A. E. (2012) Collisional facilitation of aqueous alteration of CM and CV carbonaceous chondrites. *Geochim. Cosmochim. Acta* **90**, 181–194.

Rubin A. E. (2013) An amoeboid olivine inclusion (AOI) in CK3 NWA 1559, comparison to AOIs in CV3 Allende, and the origin of AOIs in CK and CV chondrites. *Meteorit. Planet. Sci.* **48**, in press.

Rubin A. E., Wang D., Kallemeyn G. W. and Wasson J. T. (1988) The Ningqiang meteorite: classification and petrology of an anomalous CV chondrite. *Meteoritics* **23**, 13–23.

Sakamoto N., Seto Y., Itoh S., Kuramoto K., Fujino K., Nagashima K., Krot A. N. and Yurimoto H. (2007) Remnants of the early solar system water enriched in heavy oxygen isotopes. *Science* **317**, 231–233.

Schrader D. L., Franchi I. A., Connolly H. C., Greenwood R. C., Lauretta D. S. and Gibson J. M. (2011) The formation and alteration of the Renazzo-like carbonaceous chondrites I: implications of bulk-oxygen isotopic composition. *Geochim. Cosmochim. Acta* **75**, 308–325.

Scott E. R. D., Keil K. and Stöffler D. (1992) Shock metamorphism of carbonaceous chondrites. *Geochim. Cosmochim. Acta* **56**, 4281–4293.

Smith C. L. and Russell S. S. (2003) Dar al Gani 431: unraveling nebular and parent body processes. *Meteorit. Planet. Sci*. **38**, #5222 (abstr.).

Tandon S. N. and Wasson J. T. (1968) Gallium, germanium, indium and iridium variations in a suite of L-group chondrites. *Geochim. Cosmochim. Acta* **32**, 1087–1110.

Ulff-Møller F., Rasmussen K. L. and Grundvig S. (1993) Mundrabilla 012: a new CV2(?) chondrite find from Southwest Australia (abstract). *Meteoritics* **28**, 451–452.

Wasson J. T. (2005) Loss of highly volatile elements from ordinary chondrites during impact heating. *Meteorit. Planet. Sci.* **40**, A166.

Wasson J. T. and Kallemeyn G. W. (1988) Compositions of chondrites. *Philos. Trans. R. Soc. Lond.* **A325**, 535–544.

Weisberg M. K., Prinz M., Clayton R. N. and Mayeda T. K. (1997) CV3 chondrites: three subgroups, not two (abstract). *Meteorit. Planet. Sci.* **32**, A138–A139.

Weisberg M. K. and Prinz M. (1998) Fayalitic olivine in CV3 chondrite matrix and dark inclusions: a nebular origin. *Meteorit. Planet. Sci.* **33**, 1087–1099.

Weisberg M. K., Prinz M., Zolensky M. E., Clayton R. N., Mayeda T. K. and Ebihara M. (1996) Ningqiang and its relationship to oxidized CV3 chondrites (abstract). *Meteorit. Planet. Sci.* **31**, A150–A151.

Weiss B. P., Gattacceca J., Stanley S., Rochette P. and Christensen U. R. (2010) Paleomagnetic records of meteorites and early planetary differentiation. *Space Sci. Rev.* **152**, 341–390.

Zähringer J. (1966) Primordial argon and the metamorphism of chondrites. *Earth Planet. Sci. Lett.* **1**, 379–382.

Zipfel J., Palme H., Clayton R. N., Mayeda T. K., Spettel B. and Wolf D. (2000) Dar al Gani 431: a new anomalous CK3 chondrite? (abstract). *Lunar Planet. Sci*. **31**, 1668 pdf.

Associate editor: Sara S. Russell